Chin. J. Astron. Astrophys. Vol. 6 (2006), No. 4, 396–410
(*http://www.chjaa.org*)

Chinese Journal of
Astronomy and
Astrophysics

Estimating Black Hole Masses of AGNs using Ultraviolet Emission Line Properties *

Min-Zhi Kong[1,2], Xue-Bing Wu[2], Ran Wang[2] and Jin-Lin Han[1]

[1] National Astronomical Observatories, Chinese Academy of Sciences, Beijing 100012; *kmz@bao.ac.cn*
[2] Department of Astronomy, Peking University, Beijing 100871

Received 2005 December 18; accepted 2006 April 5

Abstract Based on measured broad line region sizes in the reverberation-mapping AGN sample, two new empirical relations are introduced to estimate the central black hole masses of radio-loud high-redshift ($z > 0.5$) AGNs. First, using the archival IUE/HST spectroscopy data at UV band for the reverberation-mapping objects, we obtained two new empirical relations between the BLR size and Mg II/C IV emission line luminosity. Secondly, using the newly determined black hole masses of the reverberation-mapping sample as calibration, we found two new relationships for determining the black hole mass with the full width at half maximum and the luminosity of Mg II/C IV line. We then apply the relations to estimate the black hole masses of the AGNs in the Large Bright Quasar Survey and a sample of radio-loud quasars. For the objects with small radio-loudness, the black hole mass estimated using the $R_{\rm BLR}$-$L_{\rm Mg\,II/C\,IV}$ relation is consistent with that from the $R_{\rm BLR}$-$L_{3000\,\mathring{\rm A}/1350\,\mathring{\rm A}}$ relation. For radio-loud AGNs, however, the mass estimated from the $R_{\rm BLR}$-$L_{\rm Mg\,II/C\,IV}$ relation is systematically lower than that from the continuum luminosity $L_{3000\,\mathring{\rm A}/1350\,\mathring{\rm A}}$. Because jets could have significant contributions to the UV/optical continuum luminosity of radio-loud AGNs, we emphasize once again that for radio-loud AGNs, the emission line luminosity may be a better tracer of the ionizing luminosity than the continuum luminosity, so that the relations between the BLR size and UV emission line luminosities should be used to estimate the black hole masses of high redshift radio-loud AGNs.

Key words: galaxies: nucleus — galaxies: high-redshift — quasars: emission lines — ultraviolet: galaxies

1 INTRODUCTION

Black hole masses of high-redshift AGNs ($z \gtrsim 1$) are essential for understand the early history of the universe and the formation of supermassive black holes. The mass of a black hole can be estimated with $M_{\rm BH} \sim R_{\rm BLR}\,V^2/G$, if we assume that the gas around a black hole is virialized. Here V is the characteristic velocity of BLR gas at distance $R_{\rm BLR}$ from the center of a AGN (Peterson & Wandel 1999; Peterson 1993), and G is the gravitational constant. The velocity can be estimated from $V_{\rm FWHM}$ (full width at half maximum) of the emission lines. For randomly distributed BLR clouds, $V = (\sqrt{3}/2)V_{\rm FWHM}$. The exact scale factor between V and $V_{\rm FWHM}$ depends on the structure, kinematics, and orientation of the BLR

* Supported by the National Natural Science Foundation of China.

(Peterson & Wandel 1999, 2000; McLure & Dunlop 2001; Wu & Han et al. 2001; Zhang & Wu 2002). In practical units, the virial mass of a black hole can thus be expressed in the form (see Kaspi et al. 2000),

$$M_{\rm BH} = 1.464 \times 10^5 \left(\frac{R_{\rm BLR}}{\rm lt-days}\right) \left(\frac{V_{\rm FWHM}}{10^3\,{\rm km\,s^{-1}}}\right)^2 M_\odot.$$

The reverberation mapping technique is the most important method to study the geometry and kinematics of gas in BLR (Blandford & McKee 1982; Peterson 1993, 1999, 2000; Horne et al. 2004). The BLR size, $R_{\rm BLR}$, can be deduced from the time delay in the variations of the broad emission lines, often the Hβ emission line (see Peterson et al. 2004 and references therein), relative to the ionizing continuum. In principle, this technique can be applied to any AGN; in practice, monitoring the AGNs for time delay is very time-consuming as the time scale can be of weeks, months or even years. Up to now, only 20 Seyfert 1 galaxies and 17 nearby quasars (Kaspi et al. 2000; Wandel et al. 1999; Peterson et al. 1998; Santos-Lleo et al. 2001) have been well monitored in the reverberation-mapping studies.

To ease the problem, Kaspi et al. (2000) successfully obtained an empirical relation between the BLR size of the AGN from the reverberation mapping sample and the optical continuum luminosity at 5100 Å (the $R_{\rm BLR}$-λL_λ (5100 Å) relation), which can be used to estimate BLR size. Peterson et al. (2004) recently have re-analyzed the reverberation mapping data for 35 AGNs (after PG 1351+640 and PG 1704+608 were omitted) and obtained improved time delays and hence improved estimates of BLR sizes and black hole masses. Using the improved BLR sizes in Peterson et al. (2004) and the new cosmological model, Kaspi et al. (2005) recently investigated the relation between BLR size the Hβ luminosity and the continuum at 5100 Å, 1450 Å, 1350 Å and 2–10 keV. Specifically, they found $R_{\rm BLR} \propto \lambda L_\lambda (5100\,{\rm \AA})^{0.67\pm0.05}$ with an intrinsic scatter of about 40%. The mass of black hole of a low-redshift ($z \lesssim 0.8$) AGN can thus be easily estimated using the above relation on $R_{\rm BLR}$ and $V_{\rm FWHM}$ (Laor 2000; McLure & Dunlop et al. 2001; Wandel 2002; Wu & Liu 2004). For objects at higher redshifts ($0.8 \lesssim z \lesssim 2.5$), as McLure & Jarvis (2002) stated, the $V_{\rm FWHM}$ of Mg II can be substituted for the $V_{\rm FWHM}$ of Hβ, mainly because they both are strong, fully permitted and low-ionization lines with similar ionization potentials and are emitted at approximately the same radius from the central ionizing source. It is not surprising that the FWHM values for Mg II and Hβ are very closely related for reverberation mapping objects. McLure & Jarvis (2002) obtained a relation between $R_{\rm BLR}$ from Hβ time lag and the continuum luminosity λL_λ(3000 Å). Note, however, the spectrum near 3000 Å is seriously contaminated by the blended Fe II and the Balmer continuum, so it is important to remove their effects when measuring the FWHM of Mg II. The Fe II emission can be removed from the continuum by model-fitting (McLure & Dunlop 2004), while the Balmer continuum contribution is not obvious in the residual spectrum and is difficult to remove. For two AGN samples, the LBQS (Forster et al. 2001) and the Molonglo quasar sample (Kapahi et al. 1998), McLure & Jarvis (2002) calculated the black hole masses using the two relations, $R_{\rm BLR}$-λL_λ(5100 Å) and $R_{\rm BLR}$-λL_λ(3000 Å), and found that results agree well with each other.

For one object, NGC 5548, Peterson & Wandel (1999) found from the time delay of different emission lines that the same virial relationship exists for lines emitted at different distances from the central black hole, such as Hβ, C IV λ1549 and HeII λ1640. Similar results have been obtained also for NGC 7469 and 3C 390.3 (Peterson & Wandel 2000). This suggests a possibility to determine the black hole mass using lines and/or the continuum luminosity at short wavelengths around C IV λ1549 (Vestergaard 2002). To estimate the velocity, as Vestergaard (2002) pointed out, the FWHM of C IV can be used because the line is available for a large redshift range between $z \sim 1-5$ and not much affected by strong absorption lines and the Fe II emission. To estimate $R_{\rm BLR}$, Kaspi et al. (2005) has obtained the $R_{\rm BLR}$-λL_λ(1350 Å) and $R_{\rm BLR}$-λL_λ(1450 Å) relations with a power index about 0.55 ± 0.05. Using the $R_{\rm BLR}({\rm H}_\beta)$-$L$ relation and the FWHM of C IV, one can estimate the black hole mass. The mass estimates can be calibrated using the reverberation mapping results since the BLR size of C IV and Hβ are probably different.

In most cases, the observed continuum luminosity of an AGN is mainly contributed by its nucleus, but some fraction of the continuum comes from the nonthermal emission of jets and the host galaxy. Especially for radio-loud quasars and BL Lac objects, jets could contribute significantly to the continuum radiation. Jet emission has so far been detected in all kinds of radio sources at optical/UV/X-ray/γ-ray bands (Jester 2003). More than 10 UV/optical jets have been found (O'Dea et al. 1999; Scarpa & Urry 2002; Parma et al. 2003; Scarpa et al. 1999). To diminish the jet contribution, as well as the continuum radiation from host

galaxies (though it is much weaker than the AGN), the line luminosity should be used to deduce the $R_{\rm BLR}$-L relation. Wu et al. (2004) have suggested a new relation between the BLR size and the Hβ emission line luminosity, and found that, for radio-loud AGNs, black hole masses estimated using such a new relation are systematically lower than those derived using the $R_{\rm BLR}$-λL_λ(5100 Å) relation. We noticed that the relations for $R_{\rm BLR}$ with the continuum luminosity, as obtained in Kaspi et al. (2005), were deduced from the 35 reverberation mapping AGNs, most of which are radio-quiet objects: only five, including PG 1704+608, have radio-loudness greater than 10 and only one, PG 1226+023 (3C 273), has radio-loudness greater than 1000 (see Nelson 2000). Therefore, the presence of a few radio-loud objects has only a minor effect on the R-L relation. The R-L relation derived from the reverberation mapping AGN sample therefore is not the best to estimate black hole masses of radio-loud objects for these reasons.

Like the Hβ line, the Mg II, and C IV line luminosities may be better tracers of the ionizing luminosity for radio-loud AGNs than the UV continuum luminosities. Although the detailed line radiation mechanisms are different, with Hβ being a recombination line and Mg II, C IV being collisionally excited lines, these three lines are all permitted lines produced by the photo-ionization process. Therefore, we expect that the luminosities of these lines can all trace the ionizing luminosity with, of course, different calibration factors. In fact, we have investigated the correlations between the Mg II, C IV line luminosities and the continuum luminosities or the Hβ line luminosity for the reverberation mapping AGNs, and found that the correlation coefficients are all greater than 0.9.

The main purpose of this work is to find relations between the BLR size and the Mg II, C IV emission line luminosity which can be used to estimate the black hole mass for high-redshift radio-loud AGNs. We will compare the black hole masses obtained using, respectively, the relation between the BLR size and the UV line luminosity, and that between the BLR size and the UV continuum luminosity, and then examine whether or not the black hole masses for radio-loud high-redshift objects are systematically overestimated using the UV continuum luminosity.

In Section 2, we present the spectral measurements of the Mg II and C IV emission lines obtained from archival UV data of *IUE/HST* observations for the reverberation-mapping AGNs. In Section 3, we investigate the relations between the BLR size and Mg II, C IV emission line luminosity using data of the reverberation-mapping AGNs. In Section 4, we apply the relations to other AGN samples for black hole mass estimation, and compare the black hole masses obtained by using different relations. We present our conclusions and discussion in Section 5.

Throughout the paper, a cosmological model, with $H_0 = 70\,{\rm km\,s^{-1}\,Mpc^{-1}}$, $\Omega_\Lambda = 0.7$, and $\Omega_{\rm M} = 0.3$, has been adopted.

2 DATA FOR THE REVERBERATION-MAPPING AGNS

To investigate possible relations between the BLR size and the Mg II, C IV emission line luminosities, we collected the data for the reverberation-mapping AGNs. We take the average BLR size values for 35 AGNs in Peterson et al. (2004) obtained from the time delay of the Hβ line. There is no systematically measurements of the luminosities of Mg II and C IV emission lines for the reverberation-mapping AGNs in the literature. We have measured them ourselves using the UV spectra from the *IUE* or *HST* archive. The spectra of most objects are available from *IUE*, and a few from *HST*. We measured the Mg II emission lines for 27 objects and C IV emission lines for 33 objects.

The data reduction consists of several steps. First, all the AGN spectra were extinction-corrected following a method given by Cardelli et al. (1989) and shifted to the rest frame using the IRAF software. Secondly, iron emission features in each spectrum were subtracted and the continuum was fitted with a power-law. Finally, the FWHM and the flux of Mg II and C IV emission lines were measured.

2.1 Iron Emission Subtraction and Continuum Fitting

Without subtraction of iron emission in UV/optical spectra of AGNs, the accuracy of measurements of the emission lines as well as the continua (Boroson & Green 1992; Corbin & Boroson 1996; Vestergaard & Wilkes 2001) would be limited, particularly the Mg II profile because it is often blended with relatively strong Fe II around 2800 Å.

Assuming the relative strengths of the iron lines (i.e., a template) are the same for all AGNs, Boroson & Green (1992) have developed a method to fit and remove the iron lines in the optical spectra (in the rest frame) of quasars. Vestergaard & Wilkes (2001) developed an iron template in the UV band from 1250 Å to 3090 Å (in the rest frame) using *HST* spectra of a narrow line Seyfert galaxy, I Zwicky 1, which has rich iron emission lines. They found that the template works well for eliminating the iron emissions from spectra of a few quasars. We followed the same procedures as Vestergaard & Wilkes (2001) to subtract the iron emission using their iron template, and to fit simultaneously a power law to several continuum windows from 1000 Å to 3100 Å without obvious emission lines or Fe II emissions (see table 2 from Kuraszkiewicz et al. 2002). We finally determined the flux at 3000 Å or 1350 Å from the iron-subtracted spectrum.

2.2 C IV and Mg II Emission Line Measurements

Now we try to obtain the emission line properties from the clean spectrum from which both the iron emissions and the fitted continuum have been subtracted.

We normally use only one Gaussian component to fit the C IV/Mg II line profile and measure the FWHM, if there is no an obvious narrow component. One component usually can provide a good description of line profile, especially for Mg II. However, if an absorption line is blended with C IV or Mg II lines, such as in NGC 4151, PG 1411+442, another Gaussian absorption component is added in the fitting. We ignore the asymmetry of C IV profiles often seen in the subtracted spectra, which may be induced by a relatively broad emission line such as He II $\lambda1640$ or O III] $\lambda1663$ in the red-wing or an absorption line in the blue-wing, as we believe that their net effect on the fitting result is small. We measure the line width from each spectrum, and then take the average FWHM of the Mg II and C IV emission lines (see Columns 4 and 7 in Table 1). We adopt an uncertainty of 20 percent if only one spectrum is available for an object. We did not measure the line dispersion (the second moment of the profile) as an alternative to the FWHM, which was suggested by Peterson et al. (2004) and Fromerth & Melia (2000), mainly because the line dispersion agrees well with the FWHM in the limit of a Gaussian line profile. As mentioned above, in most of our measurements one Gaussian component can provide a satisfactory fit to the line profile. We adopted the flux obtained by direct integration over the observed emission line profile of the clean-spectrum.

In Table 1, we list all the data used or obtained in this paper. The columns are object name (1), $R_{\rm BLR}$ (2) and the black hole mass (3) from Peterson et al. (2004), the FWHM (4) and luminosity (5) of MgII, the luminosity of continuum at 3000 Å (6), the FWHM (7) and luminosity (8) of C IV, the continuum luminosity at 3000 Å (9). Data from column (4) to column (9) are our measurements (see the following sections), and the number of good spectra used is given in columns (10) and (11), with the source archive indicated.

3 NEW EMPIRICAL RELATIONS FOR BLACK HOLE MASS ESTIMATION

We first try to establish the relations between the BLR size and the luminosity of Mg II, C IV emission line, using the data of the reverberation mapping AGNs obtained above. These relations can be used to estimate the BLR size of high-redshift AGNs from measurements of the luminosity of Mg II and C IV emission line, which we will do in the next section. Together with the BLR velocity obtained from the line-width, the black hole masses of high-redshift AGNs can be estimated. In this section, we will also use the known masses of black holes of the reverberation mapping AGNs to "calibrate" the empirical relations.

3.1 Relationships between the BLR Size and Mg II, C IV Emission Line Luminosity Of The Reverberation AGNs

We take the value of the BLR size of the reverberation mapping sample from Peterson et al. (2004) and the UV line luminosities measured above to investigate their relations.

As shown in Fig. 1 for the Mg II line luminosities of 27 AGNs and Fig. 2 for the C IV line luminosities of 33 AGNs, the BLR size and the line luminosities are closely related, with correlation coefficients of 0.72 and 0.76, respectively. The best fitted lines with the OLS bisector method (Isobe et al. 1990) are

$$\log \frac{R_{\rm BLR}}{\rm lt.days} = (1.13 \pm 0.13) + (0.57 \pm 0.12) \log \left(\frac{L_{\rm Mg\,II}}{10^{42}\,{\rm erg\,s^{-1}}} \right), \quad (1)$$

Table 1 Parameters of Mg II and C IV Emission Lines for 35 AGNs of the Reverberation-mapping AGN Sample

Object	$R_{\rm BLR}$ (lt-days)	$M_{\rm BH}$ $10^6 M_\odot$	FWHM$_{\rm Mg\,II}$ ($\rm km\,s^{-1}$)	$L_{\rm Mg\,II}$ ($10^{42}\,\rm erg\,s^{-1}$)	$L_{3000\rm \AA}$ ($10^{44}\,\rm erg\,s^{-1}$)	FWHM$_{\rm C\,IV}$ ($\rm km\,s^{-1}$)	$L_{\rm C\,IV}$ ($10^{42}\,\rm erg\,s^{-1}$)	$L_{1350\,\rm \AA}$ ($10^{44}\,\rm erg\,s^{-1}$)	Num Mg II	Num C IV
(1)	(2)	(3)	(4)	(5)	(6)	(7)	(8)	(9)	(10)	(11)
3C 120	$38.1^{+21.3}_{-15.3}$	$55.5^{+31.4}_{-22.5}$	3740±538	22.57±2.64	10.44±2.63	4652±937	206.81±34.22	34.30±10.05	13	34
3C 390.3	$23.6^{+6.2}_{-6.7}$	287±64	8174±622	5.36±1.83	0.99±0.48	7884±1870	23.91±9.14	2.41±1.30	6	92
Akn120	$42.1^{+7.1}_{-7.1}$	150±19	5727±842	25.93±4.94	15.45±3.10	6134±603	157.83±20.76	46.75±10.21	20	37
F9	$17.4^{+3.2}_{-4.3}$	255±56	4682±547	6.31±1.38	2.94±0.93	4981±782	23.23±7.24	3.67±2.27	54	106
MRK79	$11.7^{+5.2}_{-5.2}$	52.4±14.4	5072±1014	2.09±0.42	0.80±0.24	5301±858	10.80±1.36	1.92±0.74	1	4
MRK110	$26.0^{+6.6}_{-6.6}$	25.1±6.1	2878±575	2.19±0.44	0.55±0.16	3283± 33	8.59±0.45	0.67±0.01	2	2
MRK279	$12.4^{+6.0}_{-6.0}$	34.9±9.2	5346±465	1.92±0.27	1.04±0.47	7306±853	6.63±0.91	1.06±0.44	6	16
MRK335	$14.6^{+3.0}_{-3.0}$	14.2±3.7	2700±346	1.82±0.32	1.77±0.23	3419±202	12.17±1.27	2.64±0.41	17	22
MRK509	$79.6^{+6.1}_{-5.4}$	143±12	3921±272	15.03±1.87	7.36±1.37	6138±537	78.66±7.43	13.39±2.92	33	50
MRK590	$23.2^{+7.3}_{-7.3}$	47.5±7.4	5324±1064	0.93±0.19	0.15±0.05	4477±441	10.50±7.01	0.85±0.71	1	2
MRK817	$22.6^{+9.7}_{-9.7}$	49.4±7.7	5112±601	1.69±0.12	1.07±0.04	6481±236	6.27±0.44	1.28±0.13	2	3
NGC 3227	$6.8^{+2.0}_{-2.0}$	42.2±21.4	5406±1081	0.02±0.00	0.01±0.00	. . . . .	. . . . .	. . . . .	1	0
NGC 3516	$6.7^{+6.8}_{-3.8}$	42.7±14.6	5036±900	0.19±0.05	0.15±0.05	8018±681	1.10±0.33	0.19±0.09	19	76
NGC 3783	$10.2^{+3.3}_{-2.3}$	29.8±5.4	3031±235	3.96±0.54	2.03±0.50	4320±329	40.13±5.10	8.35±2.23	97	76
NGC 4051	$5.8^{+2.6}_{-1.8}$	1.91±0.78	2273±350	0.003±0.001	0.004±0.001	4337±898	0.01±0.002	0.002±0.0004	8	19
NGC 4151	$7.3^{+5.9}_{-5.9}$	13.3±4.6	5866±1342	0.10±0.03	0.06±0.04	6939±1902	0.72±0.31	0.07±0.05	416	454
NGC 4593	$1.2^{+9.2}_{-5.3}$	$5.36^{+9.37}_{-6.95}$	3613±363	0.12±0.02	0.08±0.02	5983±939	0.37±0.09	0.05±0.02	13	25
NGC 5548	$16.2^{+5.8}_{-5.8}$	67.1±2.6	5394±288	0.97±0.12	0.36±0.10	5289±421	4.15±0.80	0.41±0.38	116	179
NGC 7469	$4.5^{+0.7}_{-0.8}$	12.2±1.4	4123±284	1.51±0.28	0.81±0.20	4402±352	4.38±0.60	1.06±0.17	11	229
PG0026+129	$111.0^{+24.1}_{-28.3}$	393±96	1714±342	8.33±1.67	19.27±5.78	7131±1426	75.22±15.04	23.28±6.98	1	1^a
PG0052+251	$89.8^{+24.5}_{-24.1}$	369±76	. . . . .	. . . . .	. . . . .	9380±690	289.44±32.21	29.74±2.25	0	2
PG0804+761	$146.9^{+18.8}_{-18.9}$	693±83	. . . . .	. . . . .	. . . . .	5276±342	134.24±20.95	29.28±4.62	0	2
PG0844+349	$3.0^{+12.4}_{-10.0}$	92.4±38.1	3759±751	4.48±0.90	4.61±1.38	4237± 60	15.56±1.42	5.77±0.08	1^a	2
PG0953+415	$150.1^{+21.6}_{-22.6}$	276±59	. . . . .	. . . . .	. . . . .	3987±797	192.41±38.48	45.61±13.68	0	1^a
PG1211+143	$93.8^{+25.6}_{-42.1}$	146±44	3569± 79	14.10±0.58	11.72±0.09	3527±365	74.81±8.33	20.09±2.00	2^a	11
PG1226+023	$306.8^{+68.5}_{-90.9}$	886±187	5874±292	155.74±33.52	115.31±31.46	5998±794	482.92±75.31	206.81±41.58	3^a	207
PG1229+204	$37.8^{+27.6}_{-15.3}$	73.2±35.2	5414±1083	11.15±2.23	3.17±0.95	4562±912	34.44±6.89	15.88±4.76	1	1
PG1307+085	$105.6^{+36.0}_{-46.6}$	440±123	. . . . .	. . . . .	. . . . .	7507±1456	98.35±13.38	12.85±4.31	0	2^{ab}
PG1411+442	$124.3^{+61.0}_{-61.7}$	443±146	3932±786	11.34±2.27	4.46±1.34	5149±1029	20.27±4.05	2.53±0.76	1^a	1
PG1426+015	$95.0^{+29.9}_{-37.1}$	1298±385	. . . . .	. . . . .	. . . . .	7063±1569	117.56±17.67	30.78±6.79	0	4
PG1613+658	$40.1^{+15.0}_{-15.2}$	279±129	. . . . .	. . . . .	. . . . .	6890±533	83.64±11.29	17.38±3.72	0	7
PG1617+175	$71.5^{+29.6}_{-33.7}$	594±138	4896±955	18.86±0.50	10.23±1.38	7452±1589	61.98±28.47	17.87±3.95	2	2
PG2130+099	$158.1^{+29.8}_{-18.7}$	457±55	3021±154	10.16±1.45	5.63±0.67	4074±54	52.21±6.18	11.14±2.20	4	3

Notes: ^{a} spectra from HST; ^{ab} one spectrum from *IUE* and the other from HST; spectra from *IUE* if not labeled.

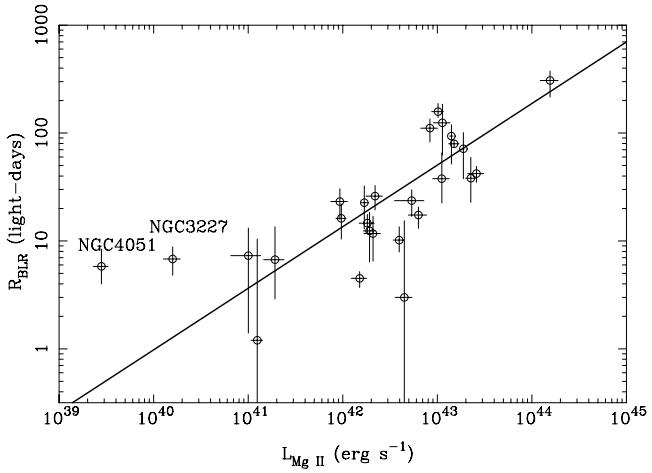

Fig. 1 BLR size, $R_{\rm BLR}$, versus Mg II emission line luminosity (λ2798 Å), $L_{\rm MgII}$, for 27 AGNs in the reverberation mapping sample for which the Mg II emission lines have been measured in Sect.2. The correlation coefficient between the two parameters is 0.72. The solid line shows an OLS bisector fit to the data (Eq. (1)), and has a slope of 0.57.

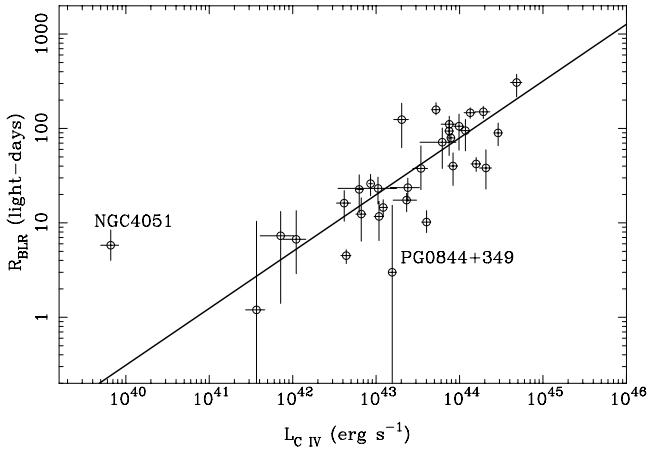

Fig. 2 Same as Fig.1, but for the C IV emission line (λ1549 Å) of 33 AGNs. The correlation coefficient is 0.76. The solid line (Eq. (2)) has a slope of 0.60.

$$\log \frac{R_{\rm BLR}}{\rm lt.days} = (0.69 \pm 0.28) + (0.60 \pm 0.16) \log \left(\frac{L_{\rm C\,IV}}{10^{42}\,{\rm erg\,s^{-1}}} \right). \quad (2)$$

Given the uncertainties, the slopes though slightly larger, are still consistent with the value 0.5 expected from a simple photo-ionization model for the BLR.

We also investigated the relations between $R_{\rm BLR}$ and the continuum luminosity $\lambda L_{3000\mathring{\rm A}}$ or $\lambda L_{1350\mathring{\rm A}}$ using our measurements in Table 1, and obtained the following relations,

$$\log \frac{R_{\rm BLR}}{\rm lt.days} = (1.27 \pm 0.10) + (0.58 \pm 0.10) \log \left(\frac{L_{3000\mathring{\rm A}}}{10^{44}\,{\rm erg\,s^{-1}}} \right), \quad (3)$$

$$\log \frac{R_{\rm BLR}}{\rm lt.days} = (1.15 \pm 0.14) + (0.56 \pm 0.12) \log \left(\frac{L_{1350\,\mathring{\rm A}}}{10^{44}\,{\rm erg\,s^{-1}}} \right). \quad (4)$$

The correlation coefficients are 0.72 and 0.75, respectively. For the relation between $R_{\rm BLR}$ and $L_{3000\,\mathring{\rm A}}$, we obtained a slope of 0.58 ± 0.10, which is consistent with the value 0.47 ± 0.05 derived by McLure & Jarvis (2002) from 34 reverberation AGNs (Kaspi et al. 2000). For the relation between $R_{\rm BLR}$ and $L_{1350\,\mathring{\rm A}}$ our slope of 0.56 ± 0.12 is well consistent with with the recent values obtained for the first time by Kaspi et al. (2005) of 0.56 ± 0.05 using the BCES method and 0.50 ± 0.04 using the $fitexy$ method. Now, there is a well-known relationship between the equivalent width of C IV broad emission line and the 1350 Å continuum luminosity of AGNs (Baldwin 1977). This so-called Baldwin-effect can be converted to $L_{\rm C\,IV} \propto L^{\alpha}_{1350\,\mathring{\rm A}}$, with a typical value of $\alpha \sim 0.4$ for an individual AGN or one of $\alpha \sim 0.83 \pm 0.04$ for a sample of AGNs (see Peterson 1997 and references therein). Using our measured $L_{1350\,\mathring{\rm A}}$ and $L_{\rm C\,IV}$ luminosities for 33 reverberation mapping AGNs, we obtained $\alpha = 0.94 \pm 0.06$. Given $R_{\rm BLR} \propto L^{0.60\pm0.16}_{\rm C\,IV}$ (Equation (2)), we easily derive $R_{\rm BLR} \propto L^{0.56}_{1350\,\mathring{\rm A}}$, shown in Equation (4).

Exclusion of four radio loud objects ($R > 10$) from the 35 AGNs in the reverberation sample in Kaspi et al. (2005), namely, 3C 120, 3C 390.3, IC 4329A and PG 1226+023, only causes a small change in the slope of R-L relations derived by Kaspi et al. (2005) and by us, because the sample is dominated by the 31 radio quiet objects (Nelson 2000).

3.2 Black Hole Mass Estimate and Calibration

The mass of a black hole can be determined by the velocity at a known radius $R_{\rm BLR}$. It is best to use the time delay in the variation of the Hβ line to determine $R_{\rm BLR}$, and the Hβ line-width for the velocity. In our estimation of the black hole mass, we will use, for $R_{\rm BLR}$, the Mg II and C IV line luminosities from Equations (1) and (2), which are "calibrated" from the the Hβ line, and for the velocity, the FWHM of the Mg II and C IV lines. Note that the time lags of flux variations of different emission lines relative to that of the UV/optical continuum are different, as shown from the measurements of the reverberation AGNs (Peterson et al. 2000, 2005; Onken & Peterson 2002; Korista et al. 1995). For example, for NGC 5548, the time lag for the C IV line is approximately half of that for the Hβ line, indicating that different emission lines are probably emitted at different distances from the center of the AGN. Therefore, we need to "calibrate" the black hole mass estimation relation when we use $R_{\rm BLR}$ and V from different emission lines.

Similar to Vestergaard (2002), we can estimate $R_{\rm BLR}$ from the line luminosity of either $L_{\rm Mg\,II}$ or $L_{\rm C\,IV}$ (see Eqs. (1) and (2)), and the velocity from the FWHM of Mg II or C IV. Finally, we estimate the black hole mass from the $R_{\rm BLR}$ and FWHM values. Using the known black hole masses of the reverberation AGNs in Peterson et al. (2004), we obtained the following "calibrated" relations (shown in Figs. 3 and 4) for black hole masses as

$$M_{\rm BH}({\rm Mg\,II}) = 2.9 \times 10^6 \left(\frac{L_{\rm Mg\,II}}{10^{42}\,{\rm erg\,s^{-1}}} \right)^{0.57\pm0.12} \left[\frac{\rm FWHM_{Mg\,II}}{1000\,{\rm km\,s^{-1}}} \right]^2 M_\odot, \quad (5)$$

$$M_{\rm BH}({\rm C\,IV}) = 4.6 \times 10^5 \left(\frac{L_{\rm C\,IV}}{10^{42}\,{\rm erg\,s^{-1}}} \right)^{0.60\pm0.16} \left[\frac{\rm FWHM_{C\,IV}}{1000\,{\rm km\,s^{-1}}} \right]^2 M_\odot. \quad (6)$$

We also tried to estimate the black hole masses using the $R_{\rm BLR}$ estimated from the continuum luminosities at 3000 Å and 1350 Å and the FWHM of Mg II and C IV lines. We obtained the following relations:

$$M_{\rm BH}(3000\,{\rm \mathring{A}}) = 3.4 \times 10^6 \left(\frac{\lambda\, L_{3000\,\mathring{\rm A}}}{10^{44}\,{\rm erg\,s^{-1}}} \right)^{0.58\pm0.10} \left[\frac{\rm FWHM_{Mg\,II}}{1000\,{\rm km\,s^{-1}}} \right]^2 M_\odot, \quad (7)$$

$$M_{\rm BH}(1350\,{\rm \mathring{A}}) = 1.3 \times 10^6 \left(\frac{\lambda\, L_{1350\,\mathring{\rm A}}}{10^{44}\,{\rm erg\,s^{-1}}} \right)^{0.56\pm0.12} \left[\frac{\rm FWHM_{C\,IV}}{1000\,{\rm km\,s^{-1}}} \right]^2 M_\odot. \quad (8)$$

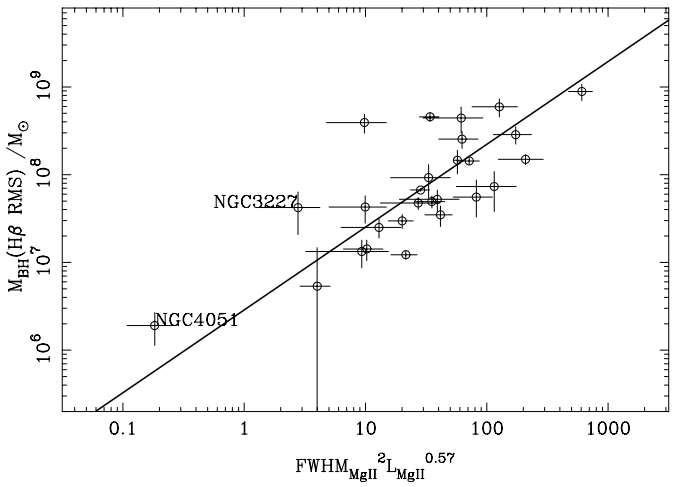

Fig. 3 Black hole masses of 27 reverberation AGNs derived from the Hβ emission line from Peterson et al. (2004) versus the "model" black hole masses from the FWHM and luminosity of the Mg II emission line. The slope of the line is 0.94 ± 0.15 from an OLS bisector fit, and the correlation coefficient is 0.76. Here the $\mathrm{FWHM_{Mg\,II}}$ is in units of 1000 km s^{-1}, and L_{MgII} in units of 10^{42} erg s^{-1}.

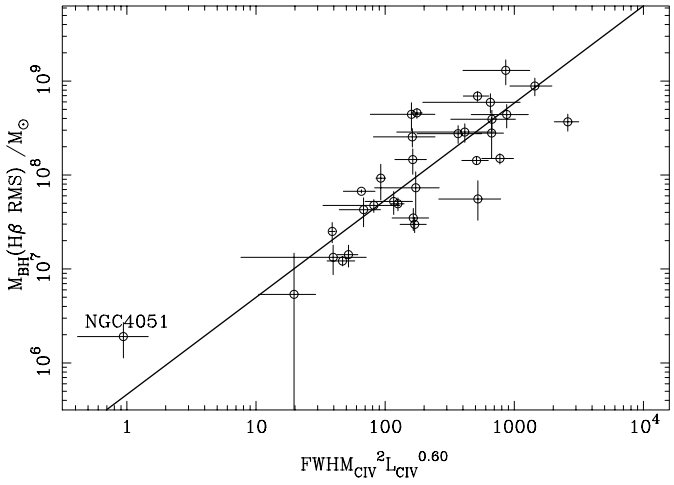

Fig. 4 Same as Fig. 3 but for the C IV emission lines of 33 reverberation AGNs. The slope of the line is 1.0 ± 0.16 from an OLS bisector fit, and the correlation coefficient is 0.86.

Note Equation (7) is similar to eq. (7) in McLure & Jarvis (2002) who obtained $M_{\mathrm{BH}}(3000\,\text{Å}) \propto L^{0.47}_{3000\,\text{Å}}\,\mathrm{FWHM^2_{Mg\,II}}$. Our slope obtained with 27 reverberation mapping AGNs is slightly larger than what they obtained with 22 objects. Equations (6) and (8) are very useful to calculate black hole masses of high redshift AGNs. Vestergaard (2002) has tried to do it using the R_{BLR} estimated from the continuum luminosity at 1350 Å and the FWHM of C IV line, adopting $R_{\mathrm{BLR}} \propto (\lambda L_{1350\,\text{Å}})^{0.7}$. The black hole mass we obtained using Equation (8) is slightly lower than what Vestergaard (2002) derived, but the values are consistent with each other within one order of magnitude.

4 BLACK HOLE MASS ESTIMATION FOR AGN SAMPLES

The relations obtained in the last section with the UV lines can be used to estimate the black hole mass of high redshift AGNs. For radio loud objects, as argued in Wu et al. (2004), jets could affect the estimate of $R_{\rm BLR}$ from the continuum luminosities. Therefore, our relations in Equations (1), (2), (5) and (6) based on the line luminosity for $R_{\rm BLR}$ should give better estimates of black hole mass for radio loud AGNs than those based on the continuum luminosities.

We apply the relations obtained above to estimate the black hole masses in two samples of AGNs. The first one is the Large Bright Quasar Survey (LBQS) sample (Forster et al. 2001; Hewett et al. 1995; Hewett et al. 2001). The second is a composite radio-loud AGN sample (Cao & Jiang 1999; Celotti et al. 1997; Barthel et al. 1990; Constantin et al. 2002).

4.1 The LBQS Sample

Forster et al. (2001) measured the optical/UV continuum and emission line properties of a homogeneous sample of 993 quasars in the LBQS, including the FWHM and equivalent width of the lines, the flux and slope of the continuum. The continuum fluxes have been Galactic extinction corrected. There are 504 objects with Mg II line measurements and 403 objects with C IV line measurement. The black hole masses of these quasars can be estimated using the relations presented in Section 3. The continuum luminosities were calculated after K-correction according to the continuum slope. The line luminosities were calculated from the equivalent width of the emission line.

We also obtained the radio-loudness for these quasars. Radio-loudness is originally defined as the ratio between the radio flux density at 5 GHz and the optical flux density at the B band (4400 Å) (Kellermann et al. 1989). We adopt B_J magnitude (Hewett et al. 1995) as an approximation of B band magnitude, which only yields an increase of 0.03 in $\log R$ on average as Hewett et al. (2001) obtained the mean $B - B_J \simeq 0.07$. The optical luminosity at 4400 Å in the rest frame of the source was calculated by assuming an optical continuum slope of 0.3 ($f_\nu \propto \nu^{-\alpha}$, Schmidt & Green 1983). For the radio data, we made cross-identifications of quasars to sources in the catalog of the NRAO VLA Sky Survey (Condon et al. 1998) and found the radio counterparts to 84 quasars with Mg II line measurements and 60 quasars with C IV line measurements. The flux density observed at 1.4 GHz was then scaled to the flux at 5 GHz in the rest frame of the source by assuming a radio continuum slope of 0.5 as an approximation. The optical and radio data so obtained were then used to calculate the radio loudness.

4.2 A Composite Sample of Radio Loud AGNs

Celotti et al. (1997) collected a radio-loud sample to investigate the relation between the broad-line emission and the central engine of AGNs. Similarly, Cao & Jiang (1999) assembled a sample of radio-loud quasars and BL Lac objects from the $1-$JY S4 and S5 radio source catalogs to investigate the relations between the broad emission line luminosity and jet power. Barthel et al. (1990) presented the optical spectra of 67 radio-loud quasars ($1.5 < z_{\rm em} < 3.8$) and measured the lines including the Mg II and C IV lines. Recently, Constantin et al. (2002) observed the C IV emission line of 34 quasars at high-redshift ($z > 4$).

Using all these data, we constructed a composite sample of radio-loud AGNs. We thus obtained 126 radio-loud AGNs with the Mg II line luminosity (86 with FWHM) and 164 AGNs with the C IV line luminosity (92 with FWHM). The radio-loudness of these AGNs were estimated using the data of 5 GHz flux density and absolute magnitude M_B available in the catalog of Véron-Cetty & Véron (2003). Optical flux densities were corrected for extinction using the A_B value available from NED, and also K-corrected assuming an optical spectral index of 0.3. Radio flux density is also K-corrected assuming a slope of 0.5 if no radio spectral index is available in literature.

4.3 Black Hole Masses from the $R_{\rm BLR}$-$L_{\rm MgII}$ and $R_{\rm BLR}$-$\lambda L_\lambda(3000\text{Å})$ Relations

We obtained 210 AGNs with the Mg II measurements from the two samples (170 of these have available Mg II FWHM). Using the relations in Equations (1), (3), (5) and (7), $M_{\rm BH}$(Mg II) and $M_{\rm BH}(3000\,\text{Å})$ can now be estimated.

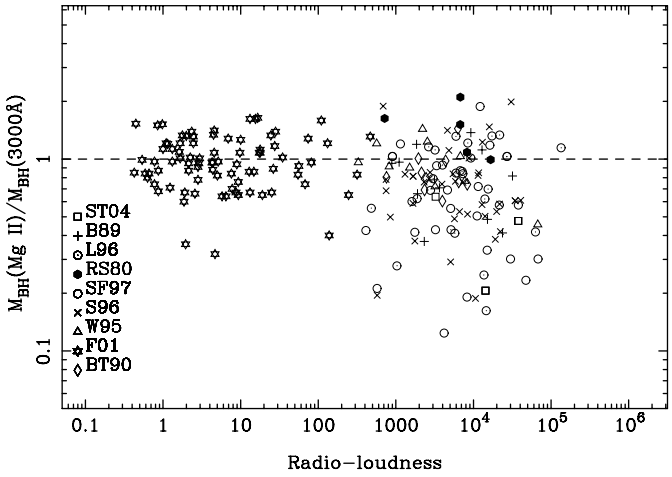

Fig. 5 Ratio of black hole masses estimated from the luminosities of Mg II and continuum versus radio-loudness for 210 AGNs. Different symbols indicate objects from different references: Sbarufatti et al. (2004, ST04); Baldwin, Wampler & Gaskell (1989, B89); Lawrence et al. (1996, L96); Richstone & Schmidt (1980, RS80); Scarpa & Falomo (1997, SF97); Stickel & Kuehr (1996, S96); Wills et al. (1995, W95); Forster et al. (2001, F01); Barthel, Tytler & Thomson (1990, BT90). The dashed line indicates identical mass estimates, and the red symbols indicate $z > 1.0$.

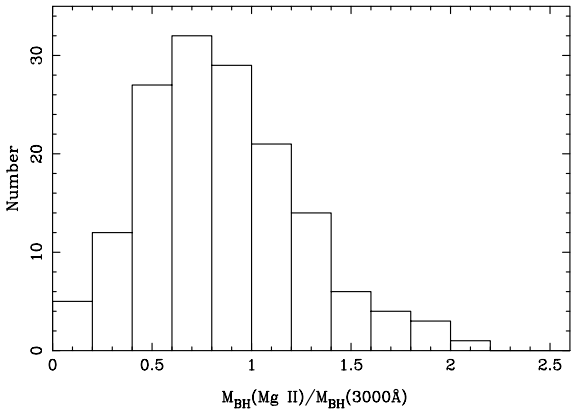

Fig. 6 Histogram of $M_{\rm Mg\,II}/M_{\rm BH}(3000\,\text{Å})$ for the 154 radio-loud AGNs ($R > 10$) shown in Figure 5. About 69% of the objects have the mass ratio less than 1. The average mass ratio is 0.80 with $\sigma = 0.1$.

Now we investigate the correlation between the mass ratio, $M_{\rm BH}$(Mg II)/$M_{\rm BH}(3000\,\text{Å})$, and the radio-loudness for the 210 AGNs. For this purpose, the FWHM data are not necessary because $M_{\rm BH}$(Mg II)/$M_{\rm BH}(3000\,\text{Å})$ calculated from Equations (5) and (7) depends only on the ratio of $L_{\rm Mg\,II}$ and $L_{3000\,\text{Å}}$. As shown in Figure 5, when the radio-loudness is small, black hole mass estimates from the line and continuum luminosities are statistically identical. As the radio-loudness increases, the mass ratio tends to be more scattered and systematically lower than 1.0. Specifically, the mass ratio is less than 0.4 for five BL Lac objects (S5 1803+78, 4C 56.27, PKS 0537–441, PKS 1144–379 and PKS 2029+121). Figure 6 shows the histogram of the $M_{\rm BH}$(Mg II)/$M_{\rm BH}(3000\,\text{Å})$ ratio of the 154 radio-loud AGNs. The mass ratio

on average is 0.80 with a deviation of $\sigma = 0.1$. This result from these two samples confirms the suggestion in Wu et al. (2004) that for radio-loud objects, especially extremely radio-loud AGNs, black hole masses should be estimated from the $R_{\rm BLR}-$line luminosity relation.

4.4 Black Hole Masses from the $R_{\rm BLR}$-$L_{\rm CIV}$ and $R_{\rm BLR}$-$\lambda L_\lambda(1350\text{Å})$ Relations

We have 224 AGNs with the C IV measurement from the two samples. Similar to the Mg II sample, we can estimate the black hole masses for 152 of the objects that have the C IV line FWHM data. Figure 7 shows the dependence of the mass ratio, $M_{\rm BH}({\rm C\,IV})/M_{\rm BH}(1350\,\text{Å})$, on the radio-loudness for all 224 AGNs, and

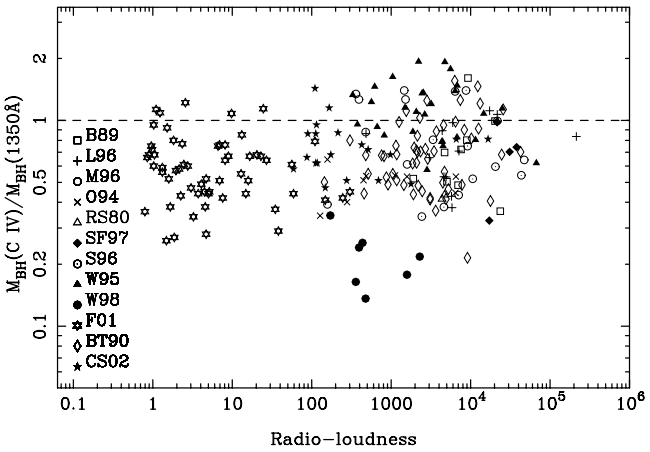

Fig. 7 Same as Fig. 5, but for 224 AGNs with measurement of C IV line. Different symbols indicate objects from different references: Baldwin, Wampler & Gaskell (1989, B89); Lawrence et al. (1996, L96); Marziani et al. (1996, M96); Osmer, Porter & Green (1994, O94); Richstone & Schmidt (1980, RS80); Scarpa & Falomo (1997, SF97); Stickel & Kuehr (1996, S96); Wills et al. (1995, W95); Wang et al. (1998, W98); Forster et al. (2001, F01); Barthel, Tytler & Thomson (1990, BT90); Constantin et al. (2002, CS02). The ratio of the black hole masses was estimated from the $R_{\rm BLR}$-$L_{\rm CIV}$ and $R_{\rm BLR}$-$\lambda L_\lambda(1350\text{Å})$ relations.

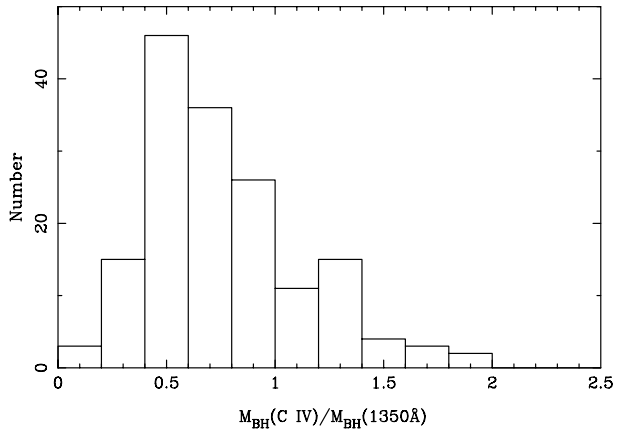

Fig. 8 Histogram of $M_{\rm BH}({\rm C\,IV})/M_{1350\,\text{Å}}$ for the 181 radio-loud AGNs ($R > 10$) shown in Fig. 7. About 70% of the objects have the mass ratio less than 1. The average mass ratio is 0.73 with $\sigma = 0.2$.

Figure 8, the histogram of $M_{\rm BH}$(C IV)/$M_{\rm BH}(1350\,\text{Å})$ for the 181 radio-loud AGNs ($R > 10$). Obviously the black hole masses estimated from the BLR size derived from the $R_{\rm BLR} - \lambda L_\lambda(1350\text{Å})$ relation are probably overestimated since 70% of the objects involved have the mass ratio less than 1. The average mass ratio is 0.73 with $\sigma = 0.2$. Thus, it is confirmed once again that the continuum luminosity is not a good indication of the ionizing luminosity because of possible jet contribution.

5 DISCUSSION AND CONCLUSIONS

Black hole masses of AGNs can be estimated relations between the BLR size and either the UV emission line luminosity or the UV continuum luminosity. We have obtained new empirical relations between the BLR size and the Mg II, C IV emission line luminosity for the reverberation-mapping AGNs (see Eqs. (1) and (2)). This enables us to estimate the black hole masses of high-redshift ($z > 0.8$) AGNs, using the luminosity and the FWHM of the UV emission lines (see Eqs. (5) and (6)).

The black hole masses so obtained were compared with those obtained using the relations between the BLR size and UV continuum luminosity (see Eqs. (7) and (8)). For radio-loud AGNs, jets contribute substantially to the continuum luminosity, therefore the black hole masses estimated from the BLR size - continuum luminosity relations (Eqs. (3) and (4)) are probably overestimated. The relation of $R_{\rm BLR}$-$L_{\rm C\,IV}$ or that of $R_{\rm BLR}$-$L_{\rm Mg\,II}$ should be a better choice.

For AGNs with Mg II line measurements, we have shown that $M_{\rm BH}$(Mg II) is very close to $M_{\rm BH}(3000\,\text{Å})$ when the radio-loudness is small. The black hole masses of radio loud AGNs estimated from the continuum luminosity are systematically larger than those from the line luminosity, confirming the suggestion by Wu et al. (2004) for $M_{\rm BH}(\text{H}\beta)/M_{\rm BH}(5100\,\text{Å})$.

For AGNs with C IV line measurements, our estimates of black hole masses of LBQS sample are slightly smaller than, but still consistent with those estimated using the relations given by Vestergaard (2002), with a slope of 0.92 and a correlation coefficient of about 0.9. The distribution of the mass ratio does not show a strong correlation with the radio-loudness. We noticed that Baskin & Laor (2005) mentioned that for high ionization emission lines like the C IV the gravitational effects on the emission line shift and profile often can not be seen, while for low ionization lines like Mg II and Hβ the effects often can be seen. If this is true, it implies that the physics may be different for the high and low ionization lines. Therefore, we should be cautious when estimating the black hole mass with the C IV emission line.

We have compared the black hole masses of LBQS quasars estimated using Equations (5) and (6) with those obtained by McLure & Jarvis (2002) and Vestergaard (2002) (see Figs. 9 and 10). Our estimates are systematically larger than those of McLure & Jarvis (2002) and smaller than those of Vestergaard (2001). This mainly comes from the different slopes of the R-L relations used in these studies.

It is important to understand the uncertainties of the data used to obtain the relations presented in this paper. These uncertainties come from the errors of the measured BLR size, the variation of emission line flux and the line FWHM, and the different inclination of the BLR. These factors have been already discussed by Wu & Liu (2004). The BLR inclination will not affect the results in this work since the black hole mass ratios $M_{\rm BH}$(Mg II)/$M_{\rm BH}(3000\,\text{Å})$ and $M_{\rm BH}$(C IV)/$M_{\rm BH}$(1350 Å) have nothing to do with inclination. The plots for the BLR size and luminosity seem to have a larger scatter for the lower luminosity objects (see Figs. 1 and 2), which can also be seen in the previous studies (Kaspi et al. 2000; Wu et al. 2004). More data of the low luminosity AGNs, especially with future reverberation mapping measurements, should be collected to improve the suggested relations.

Recently, more and more high redshift or high luminosity quasars or radio-loud ones have been found. Recent studies have used such R-L relations to obtain black hole masses of high redshift quasars with $4 \leq z \leq 6$ (Vestergaard 2004), including the most distant quasar SDSSJ$114816.64 + 525150.3$ ($z = 6.4$) (Willott, McLure & Jarvis 2003; Barth et al. 2003). However, the values of R in the R-L relations were from the reverberation mapping sample. Most of these AGNs are not very luminous and are radio-quiet AGNs. We need to beware that the black hole masses of the high redshift quasars are overestimated, especially when they are radio-loud objects. Indeed, a few high-z quasars have been already identified as radio-loud quasars (Fan et al. 2001; Momjian, Petric & Carilli 2004), therefore, further checks on the validity of suggested R-L relations for AGNs at high redshift or with large luminosity or large radio-loudness are still needed.

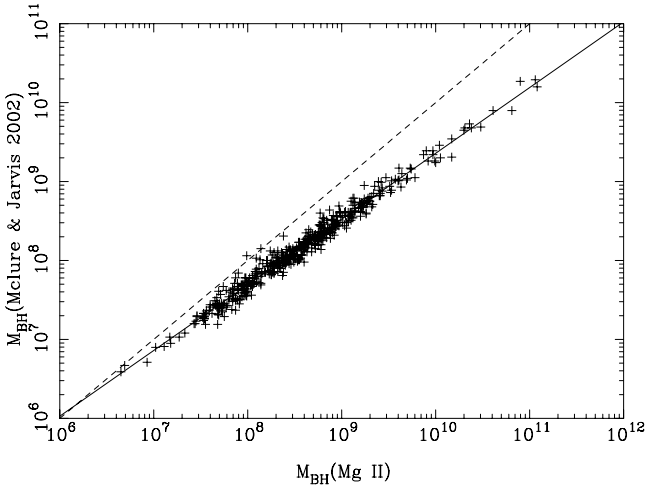

Fig. 9 Comparison of black hole masses estimated from Mg II luminosity (our Eq. (5)) and 3000 Å continuum (Mclure & Jarvis 2002) for the LBQS sample. We checked 476 objects with $1000\,\mathrm{km\ s^{-1}} < \mathrm{FWHM_{Mg\,II}} < 10\,000\,\mathrm{km\ s^{-1}}$ to avoid measurement errors or narrow line contamination. The linear fit gives a slope of 0.83 (solid line) with a correlation coefficient of 0.99. The dashed line indicates equal mass estimates.

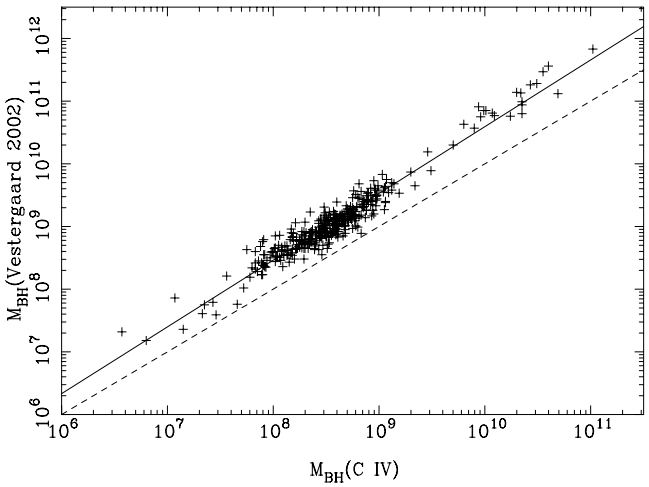

Fig. 10 Same as Fig. 9 but for black hole masses estimated from luminosity of C IV (our Eq. (6)) and continuum at 1350 Å (Vestergaard 2002) for 341 objects. The slope of the fit (solid line) is 1.06 and the correlation coefficient is 0.96.

Acknowledgements We thank Dr. Marianne Vestergaard for kindly providing us her iron template data in the UV band, and Dr. Michael Corbin for useful suggestions on the template and sending us his iron template spectra around 3000 Å. KMZ is grateful to Xiaohui Sun, Jing Wang, Yong Zhang and Yougang Wang for their numerous helps on fitting the spectra. XBW is supported by the National Natural Science Foundation of China (Nos. 10473001 and 10525313) and the Research Fund for the Doctoral program of Higher Education (No. 20050001026). JLH is supported by the National Natural Science Foundation of

China (No. 10025313) and the National Key Basic Research Science Foundation of China (G19990754) as well as the partner group of MPIfR at the National Astronomical Observatories, CAS. This work is based on the INES data from *IUE* satellite and the data from *HST* satellite partly. This research has made use of the NASA/IPAC Extragalactic Database (NED) which is operated by the Jet Propulsion Laboratory, California Institute of Technology, under contract with the National Aeronautics and Space Administration.

References

Baldwin J. A., 1977, ApJ, 214, 679
Baldwin J. A., Wampler E. J., Gaskell C. M., 1989, ApJ, 338, 630
Barth A. J., Martini P., Nelson C. H. et al., 2003, ApJ, 594, 95
Barthel P. D., Tytler D. R., Thomson B., 1990, A&AS, 82, 339
Baskin A., Laor A., 2005, MNRAS, 356, 1029
Blandford R. D., McKee C. F., 1982, ApJ, 255, 419
Boroson T. A., Green R. F., 1992, ApJS, 80, 109
Cao X. W., Jiang D. R., 1999, MNRAS , 307, 802
Cardelli J. A., Clayton G. C., Mathis J. S., 1989, ApJ, 345, 245
Celotti A., Padovani P., Ghisellini G., 1997, MNRAS, 286, 415
Condon J. J., Cotton W. D., Greisen E. W. et al., 1998, AJ, 115, 1693
Constantin A., Shields J. C., Hamann F. et al., 2002, ApJ, 565, 50
Corbin M. R., Boroson T. A., 1996, ApJS, 107, 69
Fan X. H., Narayanan V. K., Lupton R. H. et al., 2001, AJ, 122, 2833
Forster K., Green P. J., Aldcroft T. L. et al., 2001, ApJS, 134, 35
Fromerth M. J., Melia F., 2000, ApJ, 533, 172
Hewett P. C., Foltz C. B., Chaffee F. H., 1995, AJ, 109, 1498
Hewett P. C., Foltz C. B., Chaffee F. H., 2001, AJ, 122, 518
Horne K., Peterson B. M., Collier S. J. et al., 2004, PASP, 116, 465
Isobe T., Feigelson E. D., Akritas M. G. et al., 1990, ApJ, 364, 104
Jester S., 2003, New Astron. Rev., 47, 427
Kapahi V. K., Athreya R. M., Subrahmanya C. R. et al., 1998, ApJS, 118, 327
Kaspi S., Smith P. S., Netzer H. et al., 2000, ApJ, 533, 631
Kaspi S., Maoz D., Netzer H. et al., 2005, ApJ, 629, 61
Kellermann K. I., Sramek R., Schmidt M. et al., 1989, AJ, 98, 1195
Korista K. T., Alloin D., Barr P. et al., 1995, ApJS, 97, 285
Kuraszkiewicz J. K., Green P. J., Forster K. et al., 2002, ApJS, 143, 257
Laor A., 2000, ApJ, 543, L111
Lawrence C. R., Zucker J. R., Readhead A. C. S. et al., 1996, ApJS, 107, 541
Marziani P., Sulentic J. W., Dultzin-Hacyan D. et al., 1996, ApJS, 104, 37
McLure R. J., Dunlop J. S., 2001, MNRAS , 327, 199
McLure R. J., Jarvis M. J., 2002, MNRAS , 337, 109
McLure R. J., Dunlop J. S., 2004, MNRAS , 352, 1390
Momjian E., Petric A., Carilli C. L., 2004, AJ, 127, 587
Nelson C. H., 2000, ApJ, 544, L91
O'Dea C. P., De Vries W., Biretta J. A. et al., 1999, AJ, 117, 1143
Onken C. A., Peterson B. M., ApJ, 2002, 572, 746
Osmer P. S., Porter A. C., Green R. F., 1994, ApJ, 436, 678
Parma P., De Ruiter H. R., Capetti A. et al., 2003, A&A, 397, 127
Peterson B. M., 1993, PASP, 105, 247
Peterson B. M., 1997, An Introduction to Active Galactic Nuclei, Cambridge, p.91
Peterson B. M., Wanders I., Bertram R. et al., 1998, ApJ, 501, 82
Peterson B. M., Wandel A., 1999, ApJ, 521, L95
Peterson B. M., Wandel A., 2000, ApJ, 540, L13
Peterson B. M., Berlind P., Bertram R. et al., 2002, ApJ, 581, 197
Peterson B. M., Ferrarese L., Gilbert K. M. et al., 2004, ApJ, 613, 682

Richstone D. O., Schmidt M., 1980, ApJ, 235, 361
Santos-Lleo M., Clavel J., Schulz B. et al., 2001, A&A, 369, 57
Sbarufatti R., Treves A., Falomo R. et al., 2005, AJ, 129, 559
Scarpa R., Falomo R., 1997, A&A, 325, 109
Scarpa R., Urry C. M., Falomo R. et al., 1999, ApJ, 526, 643
Scarpa R., Urry C. M., 2002, New Astron. Rev., 46, 405
Schmidt M., Green R. F., 1983, ApJ, 269, 352
Stickel M., Kuehr H., 1996, A&AS, 115, 11
Véron-Cetty M. P., Véron P., 2003, A&A, 412, 399
Vestergaard M., Wilkes B. J., 2001, ApJS, 134, 1
Vestergaard M., 2002, ApJ, 571,733
Vestergaard M., 2004, ApJ, 601, 676
Wandel A., Peterson B. M., Malkan M. A., 1999, ApJ, 526, 579
Wandel A., 2002, ApJ, 565, 762
Wang T.-G., Lu Y.-J., Zhou Y.-Y., 1998, ApJ, 493, 1
Wills B. J., Thompson K. L., Han M. et al., 1995, ApJ, 447, 139
Willott C. J., McLure R. J., Jarvis M. J., ApJ, 2003, 587, L15
Wu X.-B., Han J. L., ApJ, 2001, 561, L59
Wu X.-B., Liu F. K., ApJ, 2004, 614, 91
Wu X.-B., Wang R., Kong M. Z. et al., 2004, A&A, 424, 793
Zhang T. Z., Wu X. B., 2002, ChJAA, 2, 487